developed double eyewalls when they came close to the landmass. Although the sample is admittedly biased towards the landfalling storms, there appears to be frequent coincidence of outer eyewalls with the landfall indicating an apparent relation of land-induced effects with the formation of a double eyewall.

Like the Machilipatnam cyclone of May 1990, this cyclone slowed down as it travelled towards the coast. It appears that along with the large area dense convection the cyclones which move rather slow, or slow down while racing towards the coast develop these characteristics. All the three cyclones with multiple eyewall structure showed these characteristics whereas others which did not acquire multiple eyewall structure behaved differently.

Multiple eyewalls developed on 19 May 1999 in the Arabian Sea cyclone before landfall after the intensification had ceased. They were associated with strengthening of outer core winds after the process of landfall had already started. These eyewalls developed in the pre-super cyclonic stage when the maximum sustained wind speed was about 102 knots. In the absence of any other plausible reason, land interaction seems to be the cause for development of multiple eyewalls in this cyclone.

1. Dvorak, V. F., *Mon. Weather Rev.*, 1975, **103**, 420–430.
2. Dvorak, V. F., NOAA, Tech. Report NESDIS 11, US Department of Commerce, Washington DC, 1984, p. 47.
3. Gray, W. M., *Recent Advances in Tropical Cyclone Research from Rawinsonde Composite Analysis*, WMO Publication, 1981, p. 470.
4. Willoughby, H. E., *J. Atmos. Sci.*, 1990, **47**, 242–274.
5. Raghavan, S., Rengarajan, S. and Vardharajan, V., *Mausam*, 1980, **31**, 229–240.
6. Raghavan, S., Rengarajan, S., Ramaswami, V. and Premkumar, S. W., *Mausam*, 1989, **40**, 65–72.
7. Gupta, A. and Mohanty, U. C., *Mausam*, 1997, **48**, 273–282.
8. Kalsi, S. R., Mandal, G. S., Niranjan, S. and Gupta, A., Paper presented in Tropmet 95, 1995.
9. Kalsi, S. R., Rao, A. V. R. K., Misra, D. K., Jain, R. K. and Rao, V. R., in *Advances in Tropical Meteorology* (ed. Datta, R. K.), Concept Publishing Company, New Delhi, 1996, pp. 449–458.
10. Colon, J. A., Raman, C. R. V. and Srinivasan, V., *Indian J. Meteorol. Geophys.*, 1970, **21**, 1–22.
11. Mishra, D. K. and Gupta, G. R., *Mausam*, 1976, **27**, 285–290.
12. Kalsi, S. R., Paper presented in Tropmet 99, 1999.
13. Willoughby, H. E., Clos, J. A. and Shoreibah, M. G., *J. Atoms. Sci.*, 1982, **47**, 242–274.
14. Weatherford, C. L. and Gray, W. M., *Mon. Weather Rev.*, 1988, **116**, 1044–1056.
15. Raghavan, S., *Mausam*, 1997, **48**, 169–188.
16. Hawkins, H. F., *J. Atoms. Sci.*, 1983, **40**, 1360–1361.
17. Mandal, G. S. and Gupta, A., Proceedings ICSU/WMO Intl. Symp., Peking University Press, Beijing, China, 1993, pp. 571–581.

ACKNOWLEDGEMENT. I am indebted to Dr R. R. Kelkar, Director General of Meteorology, for encouraging to study these interesting but unusual features of multiple eyewall structure of this cyclone and for permitting to publish the same.

Received 26 July 1999; accepted 10 September 1999

Snow characterization using SSM/I data

Ramesh P. Singh*, Nrusingha C. Mishra, Prasanjeet Dash and Bijay K. Mohrana

Department of Civil Engineering, Indian Institute of Technology, Kanpur 208 016, India

Snow in the Himalayan region is a vital water resource for India. Most of the river systems of India are dependent on melting of snow during summer months, which gives substantial amount of water for agriculture and hydropower, and a boost to our development. But the changes in snow cover have direct relation to global climatic changes. It is expected that the surface and atmospheric temperatures may significantly change which may influence the snow cover over high altitude regions. Currently, much attention is being paid to the global warming trend due to the increase of greenhouse gases in the earth's atmosphere. The mapping of snow cover using optical sensors, however, suffers quite often with cloud problems. Such problems do not affect microwave remote sensing which has an added advantage of quantitative estimation of snow parameters and characterization of snow cover. In the present work, an attempt has been made to study the characteristics of brightness temperature of snow over Himalayan region using SSM/I data.

THE meteorological parameters from the ground, ocean and atmosphere have paramount importance in studying the earth's climate. The Special Sensors Microwave Imager (SSM/I) has been developed as a part of the Defence Meteorological Satellite Programme (DMSP) which was launched in 1987. Efforts have been made to characterize clouds, snow[1], surface temperature[2], rainfall over land[3], oceanic total perceptible water[4], cloud liquid water content[5], ocean surface wind speed[6], atmospheric water vapour over oceans[7], and sea ice[8]. The estimation of soil moisture and evapotranspiration fluxes from SSM/I data have also been carried out[9,10]. These studies have given an overall global picture of the brightness temperature, however, no effort has been made to explore or to use SSM/I data for the Indian region. In the past efforts have been made by Indian scientists to use microwave remote sensing data[11–14] recorded by microwave radiometer on-board *Bhaskara* satellite.

The SSM/I is on-board a sun-synchronous near polar orbiting satellite[15] (DMSP Block 5D–2 F8) since the end of June 1987. It has a seven-channels, four-frequencies radiometric system providing global observations at a constant incident angle of about 53°. The SSM/I is a conical scanning radiometer, which measures thermally emitted radiation by the earth at frequencies of 19, 22, 37 and 85 GHz. The brightness temperature (T_B) measurements have been observed for both horizontal and vertical

*For correspondence (e-mail: ramesh@iitk.ac.in)

polarizations except for the 22 GHz channel, which is only vertically polarized. The NOAA/NASA Pathfinder Program EASE-Grid Brightness temperature data have been obtained from the National Snow and Ice Data Center, Boulder, Colorado, USA. These data have been decoded and average monthly, and seasonal brightness temperature, data for the northern part of the Indian sub continent (longitude 72–83°E, latitude 30–40°N) have been extracted (Figure 1). The bounded area in Figure 1 is mostly high altitude region generally covered with snow and ice.

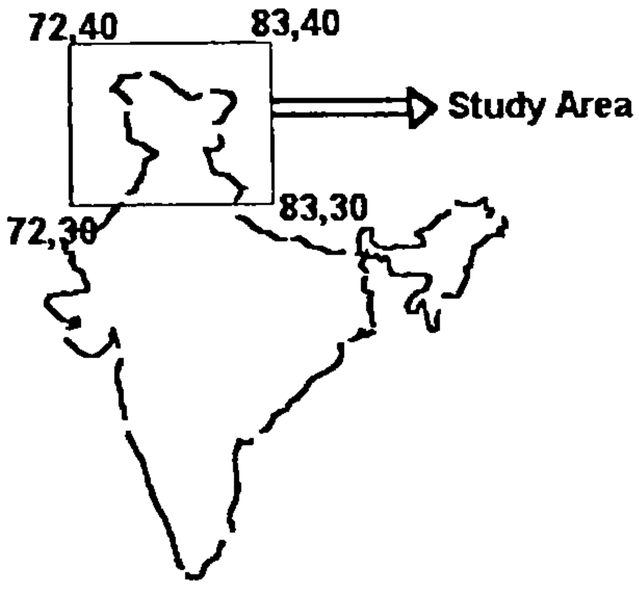

Figure 1. Location for the present study.

Figure 2 *a* shows the monthly averaged brightness temperature data at 85 GHz for horizontal polarization over the northern parts of India for July 1987–June 1988. The snow-covered region is clearly distinct from region without snow. The snow-covered region shows low brightness temperature. On the basis of the monthly averaged brightness temperature, it can be said that the onset of snowfall starts from September and continues until May. Within the snow-covered region, the variations in brightness temperature are attributed to the changes in snow thickness and physical properties of the snow. The monthly brightness temperature at 85 GHz for vertical polarization over the snow-covered region is also found to be similar.

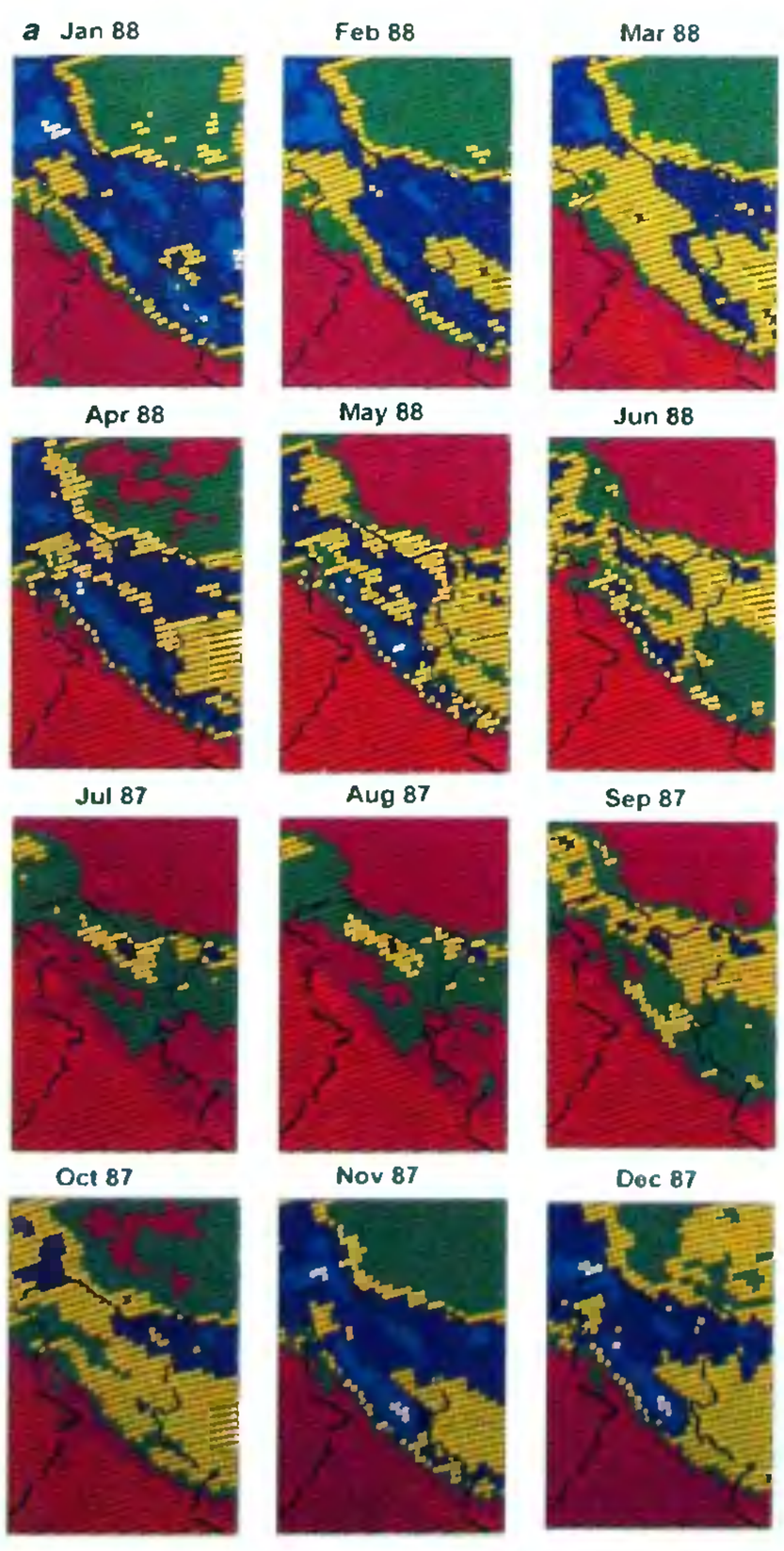

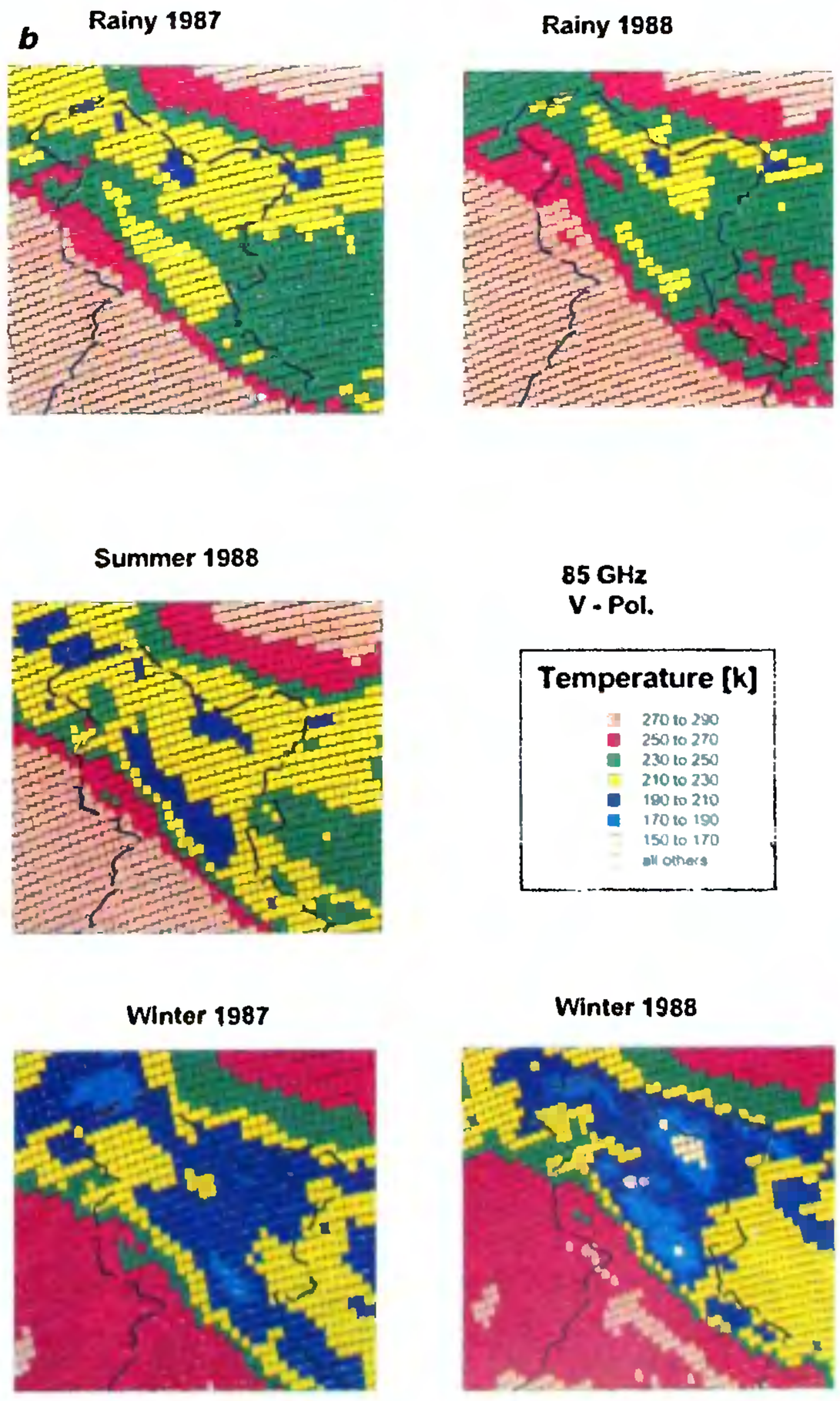

Figure 2. *a*, Monthly brightness temperature variations; *b*, Seasonal brightness temperature variations.

The brightness temperature in vertical polarization is found to be higher compared to horizontal polarization (figure is not shown).

The seasonal variations of brightness temperature image over northern India are shown in Figure 2 *b* for 85 GHz horizontal polarization. Brightness temperature is also dependent upon the thickness of snow cover. As thickness of snow increases, the microwave signals from lower surfaces are attenuated more, thus giving less brightness temperature value. The comparison of winter season during both 1988 and 1987 shows higher snow cover thickness in 1988. From Figure 2 *b* it can be concluded that larger snow cover may be present over Himalayan region during rainy and winter seasons of 1987.

The following algorithm given by Ferraro *et al.*[1] has been used to study the snow extent and thickness more precisely.

$$\mathrm{SCAT} = \mathrm{MAX}\begin{bmatrix} T_{\mathrm{B22v}} & -T_{\mathrm{B85v}} \\ T_{\mathrm{B19v}} & -T_{\mathrm{B37v}} \end{bmatrix},$$

where SCAT is the scattering index T_{B22v}, T_{B19v}, T_{B85v} and T_{B37v}, are respectively, brightness temperature in vertical polarization at 19, 22, 85 and 37 GHz. According to Ferraro *et al.*[1], if the value of SCAT is greater than or equal to 5 K, snow-covered region has been found in USA. The brightness temperature data from July 1987 to December 1988 have been considered for the analysis. The data for 85 GHz are not available from January 1989 due to failure of the sensor for which it is not possible to analyse SCAT after 1988. Using the algorithm of Ferraro *et al.*[1], we have computed SCAT over northern part of India. The criterion of SCAT greater than or equal to 5 K for mapping of the snow-covered region by Ferraro *et al.*[1] gives snow-covered region in the middle of Thar desert in Rajasthan, which is unrealistic. After numerous iterations, we have found SCAT greater than or equal to 10 K for mapping of snow cover in the Himalayan region.

Figure 3 *a* shows the variations of averaged monthly SCAT over the northern part of Indian region during 1987–1988. Higher scattering index shows the presence of snow cover. Highest SCAT of the order of 60–80 has been observed during November 1987. Sudden increase of the areal extent of the zone with scattering index in the range 20–40 is seen in October 1987. This increase of SCAT shows the onset of snowfall after 1987. During May 1988 higher scattering index is seen, which may be due to higher liquid water content in the snow. Further, the analysis of seasonal scattering index during 1987–1988 has been carried out. Higher scattering index has been observed during winter 1988 (Figure 3 *b*) compared to winter 1987, which may be due to higher snow accumulation during winter 1988. The low scattering index during 1987 rainy season compared to 1988 rainy season may be due to higher moisture content as a result of snow melting. From this observation, it can be concluded that the year 1987 was warmer compared to 1988 which can be also seen from brightness temperature maps (Figure 2 *b*).

The microwave signals emitted from the underlying ground surface propagate through the snow and are scattered by the randomly spaced snow grains in all directions. The amplitude of the microwave signals has been attenuated and they emerge at the snow–air interface. Snow absorbs very little energy from the microwave and thus, contributes very little in the form of self-emission. The microwaves suffer with scattering loss when the snow thickness increases due to which the transmission of microwave signals is further reduced. Thus, the microwave sensors measure low brightness temperature over snow-covered region. Chang *et al.*[16] have developed an algorithm to estimate snow thickness over uniform snow fields utilizing the difference in the brightness temperature between 37 and 18 GHz. The limitation of this algorithm was that it was only applicable to the snow thickness up to 1 m. Recently, Chang *et al.*[17] have modified the algorithm in order to estimate snow thickness in the high mountainous areas such as the Himalayan region. The modified algorithm of Chang *et al.*[17] for estimation of snow thickness (ST) for high mountainous areas is given below

$$\mathrm{ST} = 2.0 \times (T_{\mathrm{B18\,H}} - T_{\mathrm{B37\,H}}) - 8.0\ \mathrm{cm},$$

where T_{B18H} and T_{B37H} are brightness temperatures at 18 and 37 GHz, respectively, in horizontal polarization. The values 2.0 and – 8.0 in the above equation are the slope and intercept, respectively.

In the present work, we have used the above algorithm after minor modification for snow estimation over northern Indian. In the above algorithm, we have taken brightness temperature at 19 GHz instead of 18 GHz assuming that there will be no difference in the brightness temperature of 18 and 19 GHz which is available with SSM/I.

Figure 4 shows the monthly average plots of snow thickness over the northern part of India in the Himalayan region during August 1987–July 1998. These plots are based on the average brightness temperatures for each month. The maximum snow thickness is seen during January and February 1988 in the range 55–65 cm. However, the areal extent of the region is occupied by about four pixels in January and about two pixels in February. The larger area is covered by snow of about 35–55 cm thick in January and February. The corresponding brightness temperature of the same month at 85 GHz at horizontal polarization can be seen from Figure 2 *a* which shows lower value of the brightness temperature. This observation is similar to the theoretical analysis of Singh and Srivastav[18] who have found a decrease of brightness temperature at 37 GHz with the increasing snow thickness for snow grain size of 0.5 mm

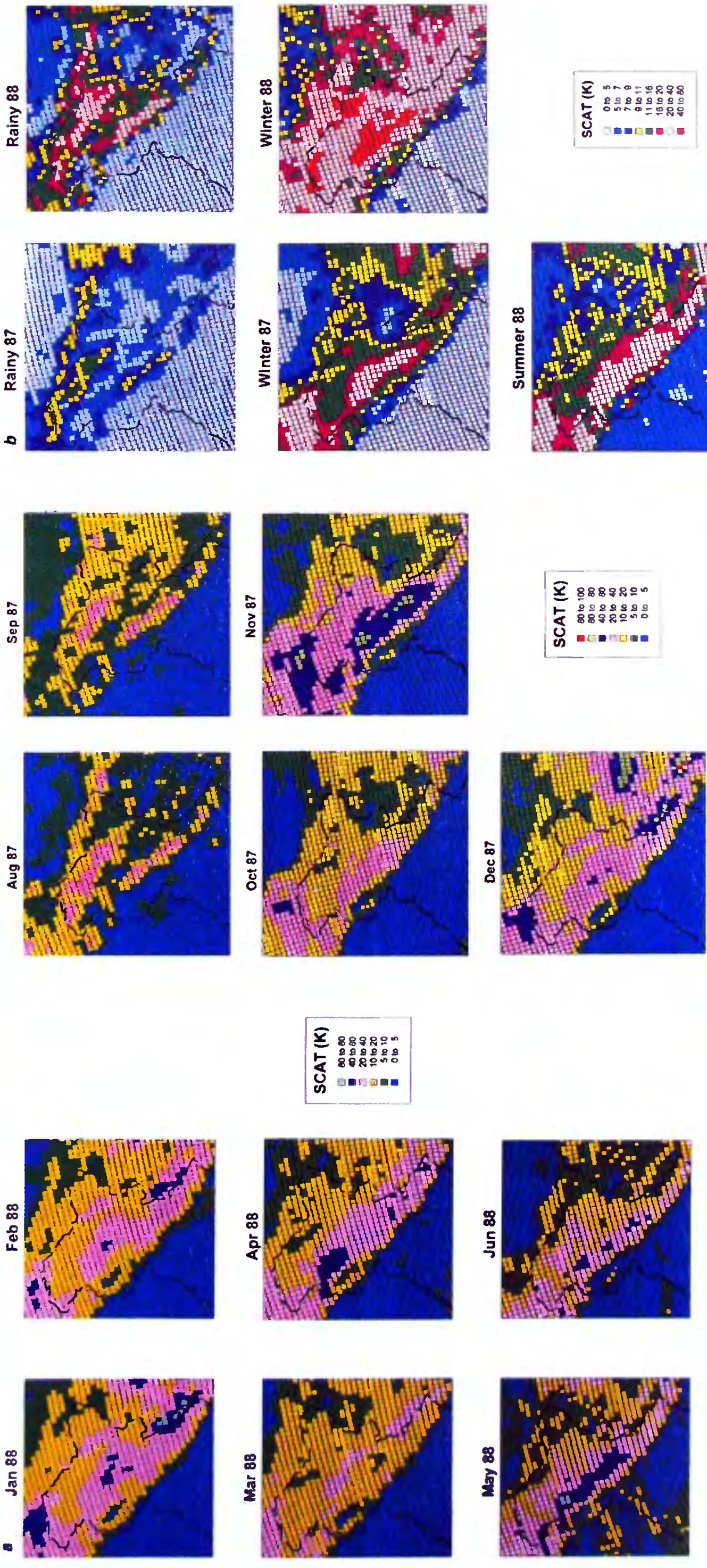

Figure 3. *a*, Monthly scattering index; *b*, Seasonal scattering index.

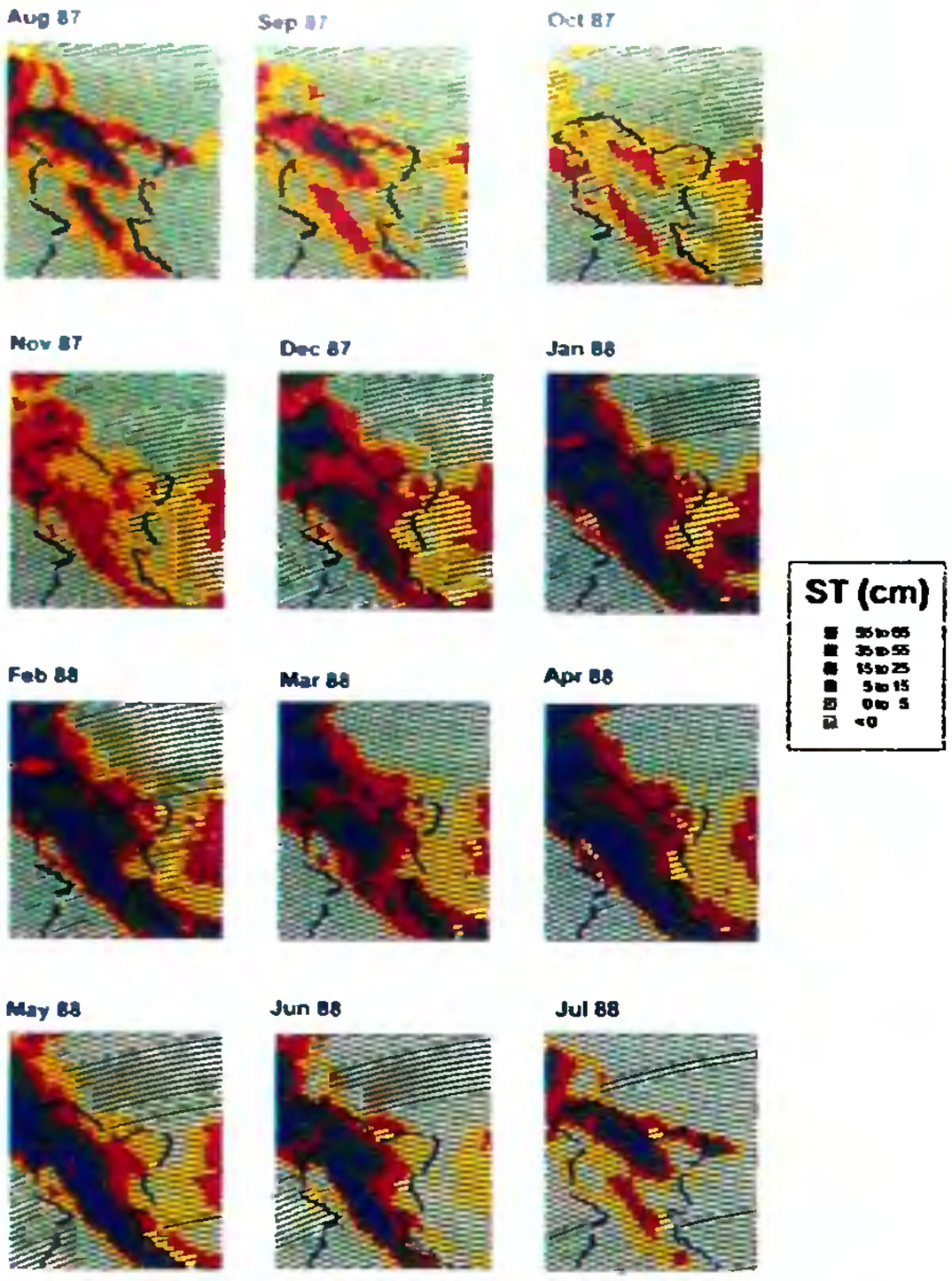

Figure 4. Time series snow thickness.

radius. The estimated snow thickness seen in Figure 4 shows a one-to-one relation with the brightness temperature observed at 85 GHz (Figure 2 *a*). From Figure 4 it is seen that the maximum area in India is covered by snow thickness (> 5 cm) during December 1987–April 1988. The present results show the potentiality of microwave remote sensing data in characterization of snow-covered region. The ground truth information is not available to the authors, such information will be of great help to validate the present result.

1. Ferraro, R. R., Fuzhong, W., Grody, N. C. and Basist, A., *Am. Meteorol. Soc.*, 1996, **77**, 891–905.
2. McFarland, M. J., Miller, R. L. and Neale, C. M. U., *IEEE Trans. Geosci. Remote Sensing*, 1990, **28**, 839–845.
3. Spencer, R. W., *J. Appl. Meteorology*, 1986, **25**, 754.
4. Alishouse, J. C., Snyder, S. A., Jennifer, V. and Ferraro, R. R., *IEEE Trans. Geosci. Remote Sensing*, 1990, **28**, 781–790.
5. Alishouse, J. C., Snider, J. B., Westwater, E. R., Swift, C. T., Ruf, C. S., Snyder, S. A., Vongsathorn, F. and Ferraro, R. R., *IEEE Trans. Geosci. Remote Sensing*, 1990, **28**, 817–822.
6. Goodberlet, M. A., Calvin, T., Swift, C. T. and Wilkerson, J. C., *IEEE Trans. Geosci. Remote Sensing*, 1990, **28**, 823–828.
7. Schluessel, P. and Emery, W. J., *Intl J. Remote Sensing*, 1990, **11**, 753–766.
8. Stephens, G. L., *J. Climate*, 1990, **3**, 634–645.
9. Lakshmi, V., Wood, E. F. and Choudhury, B. J., *Int. J. Remote Sensing*, 1997, **18**, 2763–2784.
10. Lakshmi, V., Wood, E. F. and Choudhury, B. J., *J. Geophys. Res.*, 1997, **102**, 6911–6927.
11. Pandey, P. C., *Mausam*, 1980, **31**, 561–566.
12. Pandey, P. C. and Sharma, A. K., *Mausam*, 1980, **31**, 201–208.
13. Pandey, P. C., Gohil, B. S. and Sharma, A. K., *Mausam*, 1981, **32**, 17–22.
14. Rao, K. S., Narasimha Rao, P. V., Mohan, B. K. and Murty, M. V. R., *Int. J. Remote Sensing*, 1993, **14**, 451–465.
15. Hollinger, J., *Nav. Res. Lab.*, Final Reports, Part 1 and 2, 1991, Washington, D.C.
16. Chang, A. R. C., Foster, J. L. and Hall, D. K., *Ann. Glaciol.*, 1981, **9**, 39–44.
17. Chang, A. T. C., Foster, J. L. and Hall, D. K., *Int. J. Remote Sensing*, 1990, **11**, 167–171.
18. Srivastav, S. K. and Singh, R. P., *Int. J. Remote Sensing*, 1994, **12**, 2117–2131.

ACKNOWLEDGEMENTS. The NOAA/NASA Pathfinder Program EASE-Grid Brightness temperature data were obtained from the National Snow and Ice Data Center, Boulder, Colorado, USA. Efforts made by Anupam Verma in making brightness temperature, scattering diagrams are thankfully acknowledged. We are grateful to S. S. Sarma, Director, Snow Avalanche Study Establishment, Manali and P. Mathur for their keen interest in the present work.

Received 19 March 1999; accepted 16 September 1999

Single station moment tensor inversion for focal mechanisms of Indian intra-plate earthquakes

N. Purnachandra Rao
National Geophysical Research Institute, Uppal Road, Hyderabad 500 007, India

Single station moment tensor inversion of the nearest broadband station data can be effectively used to obtain fairly accurate focal mechanism solutions for small to moderate earthquakes, as demonstrated for the 21 May 1997 Jabalpur earthquake (Mw 5.8). The method is also applied to study the 3 February 1999 Godavari valley earthquake (Mw 3.6) using broadband data of the Geoscope station, Hyderabad. A pure strike-slip solution is obtained with strike 326°, dip 88° and rake 2°. The active tectonics of the Godavari graben is studied using this result in conjunction with the mechanism of the 13 April 1969 Bhadrachalam earthquake (Mw 5.7), which also occurred in the same region. The fault planes of the two earthquakes are correlated with lineaments from Landsat images and the possiblility of a block rotation in this region is suggested.

THE Indian peninsular region is a mosaic of cratonic blocks bordered by paleo-rift valley zones. In the last few decades enhanced seismic activity has been observed even

*For correspondence. (e-mail: postmast@csngri.ren.nic.in)